Self-healing thermoplastic-toughened epoxy

A.R. Jones [a, b], C.A. Watkins [c, b], S.R. White [d, b], N.R. Sottos [c, b, *]

[a] Department of Mechanical Science and Engineering, University of Illinois at Urbana-Champaign, 1206 W. Green St., Urbana, IL, 61801, USA
[b] Beckman Institute for Advanced Science and Technology, 405 N. Mathews, Urbana, IL, 61801, USA
[c] Department of Material Science and Engineering, University of Illinois at Urbana-Champaign, 1304 W. Green St., Urbana, IL, 61801, USA
[d] Department of Aerospace Engineering, University of Illinois at Urbana-Champaign, 104 S. Wright St., Urbana, IL, 61801, USA

ARTICLE INFO

ABSTRACT

A thermoplastic resin poly(bisphenol A-co-epichlorohydrin) (PBAE) is blended with a high glass transition temperature (T_g) epoxy matrix to serve as both a toughening additive and a healing agent in combination with an encapsulated solvent. Microcapsules are coated with poly(dopamine) (PDA) to improve the thermal stability and retain the core solvent during curing at 180 °C. The fracture toughness of the high T_g epoxy (EPON 828: diamino diphenyl sulfone) is doubled by the addition of 20 wt % PBAE alone and tripled by the addition of both microcapsules and the thermoplastic phase. Self-healing is achieved with up to 57% recovery of virgin fracture toughness of the toughened epoxy. Healing performance and fracture toughness of the self-healing system remain stable after aging 30 days. The relative amount of thermoplastic phase and the presence of solvent-filled microcapsules influence the storage modulus, T_g, and healing performance of the polymer.

© 2015 Elsevier Ltd. All rights reserved.

1. Introduction

Self-healing material systems are designed to repair damage autonomously, without external intervention. Healing strategies vary from requiring some external intervention (i.e. heat or pressure) to fully autonomous systems that possess the ability to heal without intervention. To date, three primary types of healing strategies have been demonstrated including microcapsule, microvascular, and intrinsic approaches [1]. For microcapsule-based systems, healing agents are sequestered in microcapsules, which are dispersed in a host matrix. Healing is triggered by damage that ruptures the embedded microcapsules, releasing the healing agents and promoting the formation of new material within the damaged area. Microvascular systems sequester the healing agent(s) within a network of microchannels enabling continuous and/or repeated delivery during repetitive damage. Intrinsic approaches are predicated on reversible bonding (e.g. hydrogen, ionic) to provide self-healing functionality.

Previous microcapsule-based systems have lacked stability at the manufacturing temperatures common for commercial epoxies and composites (ca. 121 °C to 177 °C). For autonomous healing in high performance composites, the encapsulated healing agents must react at room temperature (during healing), but resist degradation or premature reaction during the curing of the host matrix material [2]. The selection of a healing chemistry that fulfills these two competing requirements remains a significant technical challenge. In prior work, exposure of self-healing materials to high temperatures during postcure regularly reduced healing performance. Mangun et al. [3] reported ca. 52% recovery of fracture toughness with a poly(dimethyl siloxane) healing chemistry in an epoxy matrix postcured at 100 °C for 1 h. However, a higher postcure temperature of 177 °C for 4 h reduced the healing efficiency to 28%. Jin et al. [4] achieved higher healing efficiencies (ca. 80–90%) with a multi-capsule amine/epoxy healing chemistry. However, a postcure of 121 °C for 1 h decreased healing to ca. 30–40% recovery. By tuning the healing chemistry, Jin and co-workers drastically improved performance to 90% recovery after a postcure of 150 °C for 6 h, but only achieved 60% recovery after a postcure of 177 °C for 3 h [2]. Zhang et al. [5,6] also developed an amine/epoxy healing chemistry, but observed a reduction from 60% to 40% healing efficiency after modest heat treatment temperatures (max. 80 °C). Yaun et al. [7] reported high healing efficiencies (ca. 100%) after thermal postcures (up to 180 °C for 4 h) and heat treatments (up to 250 °C) by using a high loading of amine/mercaptan and epoxy microcapsules in several different epoxy systems, with fracture toughnesses ranging from 0.5 to

1.0 MPa m$^{0.5}$.

Higher cure temperatures lead to improved mechanical properties, such as fracture toughness and elastic modulus of epoxy, which are critical for aerospace and other high performance applications. Fracture toughness is commonly increased through the addition of fillers or a thermoplastic phase [8,9]. Thermoplastic phases have also been used to repair crack damage upon heating [10]. Hayes et al. blended the thermoplastic poly(bisphenol-A-co-epichlorohydrin) (PBAE) with epoxy to achieve 70% recovery of fracture toughness after a heat treatment of 130 °C for 1 h [11]. Luo and co-workers reported fast recovery (8 min) using a poly-(caprolactone) thermoplastic additive and exposure to a temperature of 190 °C [12]. Pingkarawat et al. have reported up to 200% recovery of interlaminar fracture toughness in carbonfiber reinforced composites with poly[ethylene-co-(methacrylic acid)] (EMMA) following a heat treatment of 150 °C for 30 min [13]. Each of these systems demonstrated high healing performance, but only after external heat treatment.

In this work, we use the thermoplastic additive PBAE to simultaneously toughen and self-heal, with the aid of an encapsulated solvent, ethyl phenyl acetate, in a high temperature cured epoxy. High temperature capsule stability is achieved through the use of a high boiling point solvent, ethyl phenyl acetate (EPA), and a robust coating of poly(dopamine) (PDA) on the microcapsules. A damage event triggers the rupture of microcapsules, releasing the solvent (EPA) into the crack plane. Locally, the thermoplastic dissolves and redistributes in the damage region, followed by diffusion and eventual evaporation of the solvent. To characterize this healing event, we vary healing cycle time and thermoplastic loading. The combination of a thermoplastic additive and an encapsulated solvent is a motif that can be translated to other thermosetting matrices to achieve synergistic toughening and self-healing.

2. Experimental

2.1. Materials

Urea, ammonium chloride, resorcinol, formalin (37 wt % formaldehyde), octanol, dopamine hydrochloride, ammonium persulfate, sodium phosphate monobasic monohydrate, sodium citrate dihydrate, ethyl phenyl acetate (EPA), diamino diphenyl sulfone (DDS), and poly(bisphenol A-co-epichlorohydrin) (PBAE) were purchased from Sigma Aldrich and used as received. Ethylene maleic-co-anhydride (EMA) copolymer (ZeMac E400, Vertellus) was prepared in a 2.5% w/v aqueous solution and used as a surfactant. Desmodur L75 was generously supplied by Bayer as a polyurethane prepolymer. EPON 828 epoxy resin was purchased from Miller−Stephenson. Araldite LY 8605 epoxy resin and Aradur 8605 hardener were purchased from Huntsman.

2.2. Synthesis of microcapsules

Capsules were prepared using a double shell wall technique previously described by Caruso et al. [14]. In this technique, polyurethane prepolymer (Desmodur L75) undergoes a rapid interfacial polymerization forming the inner shell wall, which is followed by an in situ polymerization of urea and formaldehyde. An aqueous solution of surfactant (EMA) and shell wall formers (urea, ammonium chloride, and resorcinol) was prepared and the pH was adjusted to 3.5 by dropwise addition of sodium hydroxide. The core material was comprised of ethyl phenyl acetate (EPA) and 0.05 g of Desmodur L75 per mL of EPA. The core solution was then slowly added to the aqueous solution and allowed to emulsify for 20 min at 400 rpm. Formalin was added to the encapsulation mixture and the temperature of the control bath was slowly ramped to 55 °C at

1 °C/min for 4 h. After the reaction was complete, the microcapsules were recovered by filtration and sieved to be between 75 and 250 μm in diameter.

Dry microcapsules were subjected to a second process, in which a coating of poly(dopamine) (PDA) was uniformly deposited on the outer shell, following a process described by Kang et al. [15]. Ammonium persulfate was used to oxidize the catechol moieties in dopamine hydrochloride, thus producing quinine which polymerizes to form PDA. Microcapsules (3 g) were added to 36 ml of buffer solution (pH = 7.0), 0.66 g of dopamine hydrochloride, and 0.66 g of ammonium persulfate. The reaction was allowed to continue for 24 h at room temperature under agitation. Capsules were again recovered by filtration.

2.3. Characterization of microcapsules

The microcapsule size distribution was obtained by image analysis of a minimum of 200 microcapsules. Scanning electron microscopy (SEM) was used to examine shell wall morphology. The thermal stability of the microcapsules was first evaluated using thermogravimetric analysis (TGA). TGA was performed by ramping the temperature from room temperature up to 180 °C at 10 °C/min
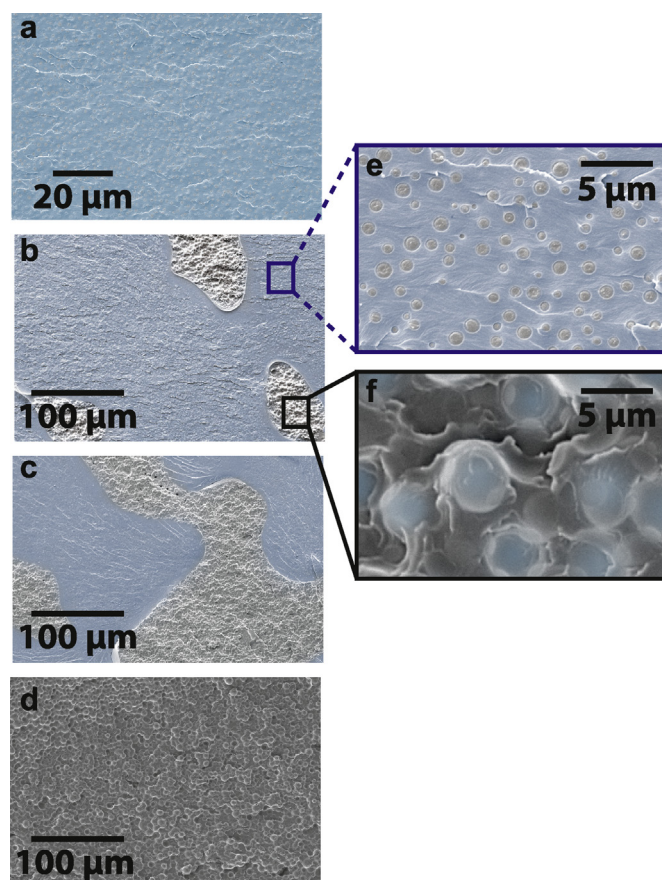
Fig. 1. Phase morphology of thermoplastic/epoxy blends. SEM images of the fracture surface morphology (epoxy = blue, PBAE = gray) with increasing wt % PBAE: (a) 10 wt % PBAE, (b) 15 wt % PBAE, (c) 20 wt % PBAE, and (d) 25 wt % PBAE. At 10 wt % PBAE, small thermoplastic particulates were dispersed in an epoxy matrix (shown at a higher magnification in (e)). As the wt % of PBAE increased, bi-continuous phase separation was observed with both thermoplastic particulates in an epoxy matrix (e) and phase inversion, consisting of epoxy regions coated with a thermoplastic matrix (f). Phase inversion increasingly dominated the surface morphology until full phase inversion was observed at 25 wt % PBAE. (For interpretation of the references to color in this figure legend, the reader is referred to the web version of this article.)
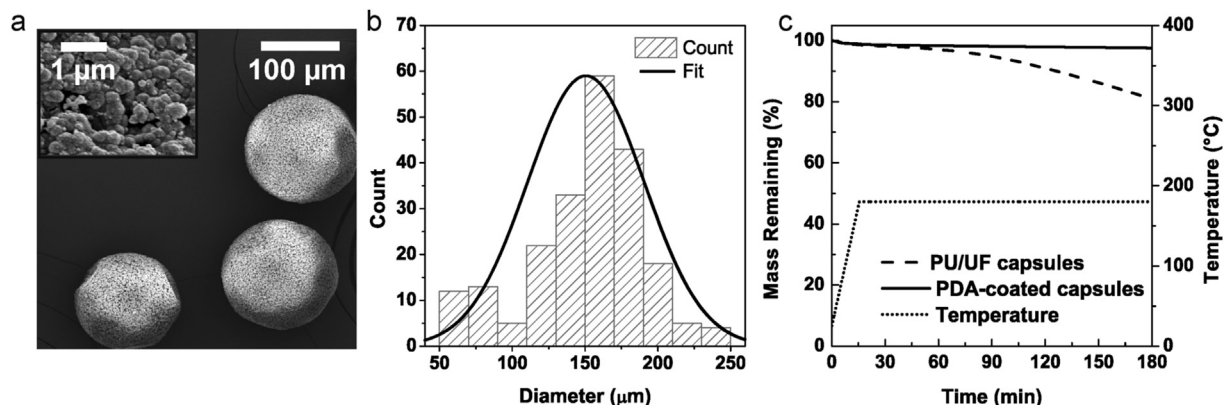
Fig. 2. Characterization of double-shell walled microcapsules with poly(dopamine) (PDA) coating. (a) SEM image of PDA-coated capsules with inset of shell wall morphology. (b) Representative size distribution of microcapsules with an average diameter of 150 μm. (c) Isothermal TGA trace showing mass loss during exposure to 180 °C for 3 h. PU/UF double shell walled microcapsules retain ca. 80% of core, while capsules with PDA coating retain nearly 100% after thermal exposure.

and holding for 3 h. Mass loss was recorded as a function of time.

For select samples, thermal stability was further analyzed by using a hot stage mounted under an optical microscope. The samples consisted of an aliquot of the microcapsule-filled thermoplastic/epoxy blend between two coverslips. The thickness of the specimens was kept constant by using 180—250 μm glass beads (McMaster-Carr) as spacers between the two coverslips. The samples were exposed to the same cure cycle as bulk polymer specimens and images were taken throughout the cure process.

2.4. Polymer blend preparation

A thermoplastic-toughened epoxy was prepared using a polymer melt-blend technique which resulted in either 10, 15, or 20 wt % PBAE in the epoxy (EPON 828: DDS). The thermoplastic (PBAE) was combined with EPON 828 at 150 °C for 4 h under vacuum and agitation (50 rpm). Once the thermoplastic/resin mixture was homogenous, a stoichiometric amount (32 pph) of resin hardener, DDS, was dissolved in the resin blend for 15 min under vacuum. In select samples, 5 wt % microcapsules were added to the polymer and slowly distributed. Then the entire mixture was placed in a vacuum oven to degas at 110 °C for 10 min. The material was poured into molds that were preheated to 150 °C. Once pouring was complete, specimens were cured at 180 °C for 1 h. Both the ramp up to 180 °C (from 150 °C) and the cool down ramp were kept constant at 1 °C/min.

## 2.5. Preparation of specimens for dynamic mechanical analysis

Dynamic mechanical analysis (TA Instruments RSA III Dynamic Mechanical Analyzer) was performed based on the ASTM Standard D5023-07 [16]. Rectangular specimens (29.0 × 8.0 × 2.0 mm) were tested in three point bending (25 mm span). The temperature was increased from 25 °C to 250 °C at 5 °C/min using a frequency of 1 Hz and a strain amplitude of 0.3%. In this work, the glass transition temperature was defined as the peak in the tangent of the phase angle (ASTM E1640-13) [17].

2.6. Preparation of fracture specimens

Fracture specimens were prepared using a localized short groove tapered double cantilever beam (TDCB) specimen (Fig. 5a)
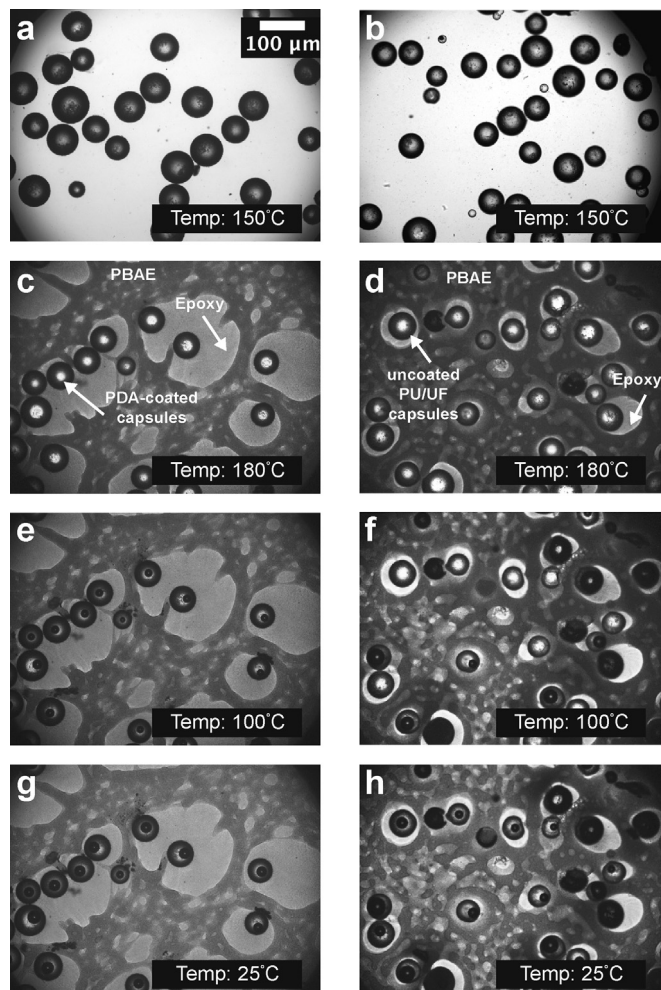
Fig. 3. Observation of PDA-coated (left) and uncoated (right) microcapsule stability during cure. The cure cycle progressed from the addition of the hardener at 150 °C (a and b) to a 1 h hold at 180 °C (c and d) followed by controlled cooling (1 °C/min) to room temperature. Microcapsule integrity is improved by the addition of a PDA coating. Voids appeared ca. 100 °C (e and f) and grew slightly larger upon reaching room temperature (g and h). We hypothesize these voids are water that diffuses into the capsule at high temperature.

a

b
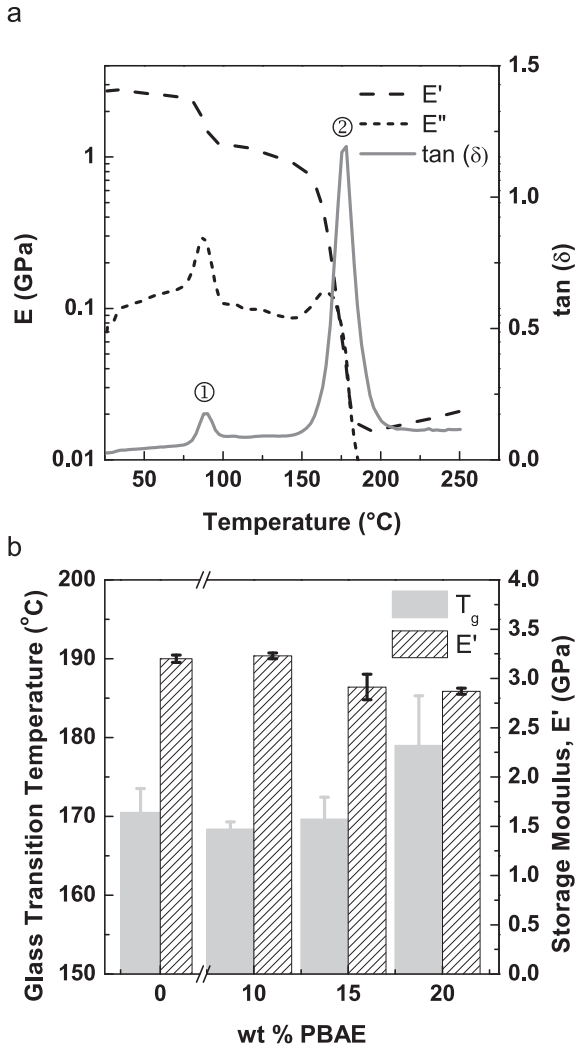
Fig. 4. Effect of PBAE content on modulus and glass transition temperature. (a) Representative DMA data for a 20 wt % PBAE specimen, where ① represents the T_g of the PBAE phase and ② denotes the T_g of the epoxy phase. (b) Average epoxy glass transition temperature (T_g) and storage modulus as a function of wt % PBAE. Error bars represent standard deviation.

as previously described by Rule et al. [16]. To prepare TDCB specimens, Aradur 8605 hardener and Araldite Y 8605 resin were mixed (35:100 by weight), degassed, poured into silicon rubber molds (with silicon rubber inserts aligned in the center of the specimen, Fig. 5a) and cured at 150 °C for 20 min. The silicone inserts were then removed and the active material (polymer blend described above) was added to the insert region.

Prior to testing, a precrack was created using a razor blade along the centerline of the specimen. Specimens were pin loaded in Mode I tension under displacement control at a loading rate of 5 μm/s until the crack arrested at the end of the grooved region. Samples were then unloaded, allowing the crack faces to come back into contact before evaluation of the healing performance.

The tapered design of the TDCB specimen geometry creates a constant compliance region. The fracture toughness, K_{Ic}, is crack length independent in that region and is calculated as:

$$K_{Ic} = \alpha P_{avg}, \tag{1}$$

where α is a geometric constant ($\alpha = 11.2 \times 10^3 \text{ m}^{-3/2}$ in this work).

2.7. Healing performance evaluation

Several sample types were used to evaluate healing performance and are summarized in Table 2. Unless otherwise stated, 20 wt % PBAE was incorporated in all samples. Self-healing samples were prepared with 5 wt % EPA-filled microcapsules and allowed to heal for a specified amount of time at 30 °C. Two different reference tests (no microcapsules) were carried-out to determine maximum healing efficiency. Specimens for type I reference tests were fabricated with either 10, 15, or 20 wt % PBAE. Healing performance was evaluated by manually injecting 5 μl of EPA into the specimens after virgin testing and allowing them to heal for a specified amount of time at 30 °C. For type II reference tests, specimens with 20 wt % PBAE were heated to 180 °C for 1 h after virgin testing to determine the recovery obtained from heat treatment alone. Three controls of the neat epoxy (EPON 828: DDS) were prepared without any thermoplastic additive to confirm that both PBAE and EPA are required for healing. Control I specimens were manually injected with 5 μl of EPA in order to mimic type I reference tests. Control II specimens were heated to 180 °C for 1 h after virgin testing to compare to the performance of type II reference samples. The last control, control III, contained 5 wt % EPA-filled microcapsules, to compare with self-healing specimens.

Healing efficiency, η, was defined as the ratio of the mode I fracture toughness of the healed test to that of the virgin test. Average healing efficiencies were calculated by averaging the value for each sample tested. For the TDCB geometry, healing efficiency simplified to the ratio of the peak loads,

$$\eta = \frac{K_{Ic,healed}}{K_{Ic,virgin}} = \frac{P_{avg,healed}}{P_{avg,virgin}}. \tag{2}$$

3. Results and discussion

3.1. Matrix morphology

The thermoplastic phase served to toughen the epoxy matrix as well as participate in crack repair. The thermoplastic-toughening effect was a result of phase separation that occurred during the cure cycle. Similar to prior work by Hedrick et al. [17], SEM micrographs, shown in Fig. 1, reveal a change in the matrix morphology as the amount of thermoplastic in the epoxy increased. Hedrick and coworkers additionally demonstrated the importance of chemical compatibility and interfacial adhesion between the thermoplastic and epoxy matrix, which motivated the selection of PBAE as the thermoplastic additive in this work. At low loadings of thermoplastic, small 1–2 μm particles of PBAE formed inside an epoxy matrix (shown in blue). As the amount of PBAE increased, a co-continuous morphology developed, consisting of thermoplastic particles in an epoxy matrix as well as isolated epoxy regions inside a thermoplastic matrix (grey). At higher loadings (≥25 wt %), complete phase inversion (continuous thermoplastic matrix with isolated epoxy regions) occurred. Only a few specimens were prepared at these loadings since viscosity was dramatically increased and specimen preparation was difficult.

3.2. Microcapsule thermal stability

An SEM image and representative size distribution of the EPA-filled microcapsules with a poly(dopamine) (PDA) coating are shown in Fig. 2. The capsules were formed with a relatively rough exterior surface due to the deposition of colloidal UF (Fig. 2a). The addition of the PDA coating did not noticeably change the
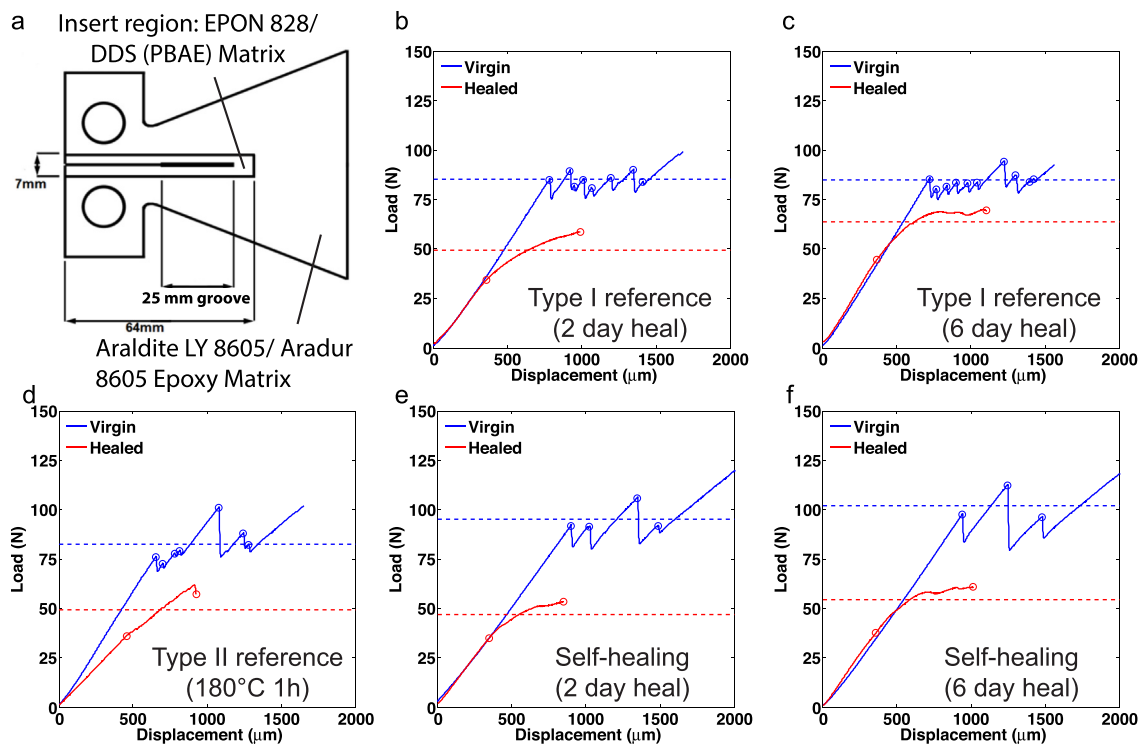
Fig. 5. Representative load–displacement curves for virgin and healed tests of specimens containing 20 wt % PBAE. (a) Schematic of TDCB specimen. (b) Representative load–displacement curves for type I reference samples injected with 5 μl of EPA and allowed to heal for 2 days and (c) 6 days. (d) Load-displacement curve for a type II reference sample exposed to a healing cycle of 180 °C for 1 h. (e) Load-displacement curve for a self-healing sample allowed to heal for 2 and (f) 6 days. Dashed lines represent the average peak loads, used to calculate healing efficiency.

Table 1
Summary of DMA results.

PBAE (wt %)	Capsule fraction (wt %)	T_g (C)	E' (GPa)
0	0	170 ± 3.0	3.2 ± 0.04
10	0	168 ± 0.9	3.2 ± 0.03
15	0	170 ± 2.8	2.9 ± 0.13
20	0	179 ± 6.3	2.9 ± 0.03
20	5	167 ± 2.3	2.6 ± 0.25

morphology of the capsule shell wall. A representative size distribution is given for the PDA-coated capsules in Fig. 2b. The capsules had an average diameter of 150 ± 40 μm.

Thermal stability of the capsules was first assessed by TGA (Fig. 2c) without exposure to the epoxy curing process. Double shell walled microcapsules retained ca. 80% core after exposure to 180 °C for 3 h. The temperature, 180 °C, was selected based on the maximum temperature observed during curing. Thermal stability was dramatically increased with the additional PDA coating. As described by Kang et al. [15], the PDA coating was formed by polymerizing dopamine hydrochloride in an aqueous solution (pH = 7.0). Nearly complete retention of core material was observed for capsules with a PDA coating (Fig. 2c) after 3 h at 180 °C.

Capsule integrity was further investigated during the cure of the thermoplastic/epoxy blend on a hot stage under an optical microscope (Fig. 3). Images at various stages of the cure cycle are

Table 2
Fracture toughness and healing performance of specimens.

Sample Type	PBAE (wt %)	Capsule wt %	Heal Time	Heal Temp. (°C)	K_{Ic}^{virgin} (MPa m$^{0.5}$)	K_{Ic}^{healed} (MPa m$^{0.5}$)	Healing Efficiency (η)
Control I	0	0	2d	30	0.40 ± 0.08	0	0
Control II	0	0	1 h	180	0.40 ± 0.08	0	0
Control III	0	5	2d	30	0.52 ± 0.03	0	0
Type I reference	10	0	2d	30	0.54 ± 0.05	0	0
Type I reference	15	0	2d	30	0.79 ± 0.04	0.41 ± 0.02	0.53 ± 0.03
Type I reference	20	0	2d	30	0.98 ± 0.06	0.60 ± 0.04	0.56 ± 0.03
Type I reference	20	0	4d	30	0.98 ± 0.06	0.68 ± 0.02	0.68 ± 0.02
Type I reference	20	0	6d	30	0.98 ± 0.06	0.68 ± 0.05	0.72 ± 0.03
Type II reference	20	0	1 h	180	0.98 ± 0.06	0.67 ± 0.08	0.68 ± 0.06
Self-healing	20	5	2d	30	1.23 ± 0.10	0.56 ± 0.04	0.46 ± 0.02
Self-healing	20	5	4d	30	1.23 ± 0.10	0.59 ± 0.01	0.48 ± 0.02
Self-healing	20	5	6d	30	1.23 ± 0.10	0.72 ± 0.03	0.57 ± 0.04
Aged-15 days	20	5	6d	30	1.19 ± 0.06	0.68 ± 0.03	0.57 ± 0.04
Aged-30 days	20	5	6d	30	1.17 ± 0.05	0.65 ± 0.03	0.56 ± 0.04

shown for both PDA-coated capsules (left) and uncoated capsules (right). The amine hardener selected for this epoxy is solid at room temperature and was dissolved at 150 °C in the thermoplastic/epoxy blend. Microcapsules were then distributed in the resin and the entire mixture was degassed for 10 min. An aliquot of this resin was deposited on a preheated glass coverslip (also at 150 °C) under the microscope (Fig. 3a, b). At this stage of the cure, the degree of cure of the epoxy was low, which allowed the thermoplastic to remain dissolved homogeneously. Also, both the PDA-coated (Fig. 3a) and uncoated (Fig. 3b) capsules appeared spherical in shape and undeformed, demonstrating that the mixing and degassing stages at high temperature did not harm the microcapsules.

The phase separation began after ca. 45 min and was completed by the end of the 1 h at 180 °C portion of the cure (Fig. 3c, d). Similar to the SEM images in Fig. 1, a bi-continuous structure was observed containing both a PBAE thermoplastic-dominant matrix region (dark grey) and an epoxy dominant region (light grey). The microcapsules preferred to reside within the epoxy-rich phase, which was attributed to the compatibility of the UF shell wall with epoxy. The PDA-coated capsules (Fig. 3c) showed no deformation while the uncoated capsules began to exhibit some wrinkling and shell wall collapse (Fig. 3d).

After the epoxy was cured for 1 h at 180 °C, the material was cooled at 1 °C/min. During cool down, a circular "void" appeared inside both types of capsules at ca. 100 °C (Fig. 3e, f). These voids grew slightly larger as the cool down progressed to room temperature (Fig. 3g, h). For PDA-coated capsules, the voids were the only feature observed (Fig. 3g), while uncoated capsules also exhibited shell wall collapse (manifest as black spheres) or wrinkling (Fig. 3h). We hypothesize the voids are actually water that diffuses as water vapor into the microcapsules during the cure process at 180 °C. Though the core solvent (EPA) is relatively hydrophobic, it is possible that trace amounts of water vapor may be soluble in EPA at elevated temperatures. As the material cools down below 100 °C, the water vapor condenses out of the EPA.

3.3. Modulus and glass transition temperature

DMA (dynamic mechanical analysis) specimens with varying wt % of PBAE were prepared to determine the modulus and the glass transition temperature of the PBAE-toughened epoxy matrix (Fig. 4 and Table 1). Representative DMA traces are shown in Fig. 4a for a specimen with 20 wt % PBAE. The storage modulus of the material remained constant until the glass transition temperature of the thermoplastic phase was reached (Fig. 4a, peak 1). A slight drop occurred with the softening of the thermoplastic phase and then a more precipitous drop at the T_g of the epoxy (ca. 180 °C, peak 2). This dual peak behavior is typical of thermoplastic-toughened epoxy systems.

The effect of increasing the PBAE content on both glass transition temperature and storage modulus is shown in Fig. 4b. The T_g increased ca. 9 °C at the highest concentration (20 wt %) of PBAE while the storage modulus decreased slightly (ca. 9%). The modest increase in glass transition temperature may be due to trace amounts of thermoplastic dissolved in the epoxy phase or the formation of a graft copolymer [18].

Specimens were also prepared with 5 wt % microcapsules for DMA testing. Both the glass transition temperature and modulus were reduced with the addition of microcapsules (Table 1), but the glass transition temperature was within experimental error of the unmodified epoxy (no PBAE, no microcapsules). Similar drops in both modulus and glass transition temperature have been observed in prior work by Moll et al. [19].

3.4. Fracture toughness and healing performance

TDCB specimens (Fig. 5a) were healed for different lengths of time at two different temperatures, 30 °C and 180 °C. Representative load−displacement curves for all sample types (with 20 wt % PBAE) are shown in Fig. 5 and a summary of all fracture testing results is given in Table 2. For all virgin tests, characteristic stick-slip crack growth was observed. The average peak load in the virgin test is denoted by a blue dashed line and was calculated from the peaks in the load−displacement data (denoted by open blue circles) in Fig. 5.

Recovery of fracture toughness for self-healing and type I reference tests was dependent on the amount of time allotted for healing. After 2 d, the healing response is nonlinear until gradually reaching a peak load, which is consistent with a drawing or tearing of the thermoplastic phase during the fracture process (Fig. 5b,e). When the healing time was increased to 6 d, the load−displacement response was more linear and near stable crack growth was observed (Fig. 5c,f). The average load in the healed test was defined as the average of the data between the beginning of deviation from the initial slope and the end of crack propagation. For consistency, the point of deviation was calculated by finding the location of 10% offset from the initial slope. The points marking the beginning and end of the averaged data are denoted by open red circles in Fig. 5. Again, the calculated average healed load is denoted by a dashed line (red).

Representative data for a type II reference specimen (with no solvent) healed at 180 °C is shown in Fig. 5d. The peak loads were on the same order of magnitude as the type I reference tests with solvent injection (healed at 30 °C). However, a significant reduction in initial slope occurred in all type II reference samples tested, suggesting only part of the virgin crack was healed.

3.4.1. Effect of thermoplastic concentration

To determine the effect of thermoplastic concentration on virgin fracture toughness and healing efficiency, we fabricated control and type I reference TDCB samples (no microcapsules) with 0, 10, 15 and 20 wt % PBAE. As the amount of thermoplastic increased, so did the virgin fracture toughness (Fig. 6). The toughening effect was due largely to the change in morphology that occurred with increasing
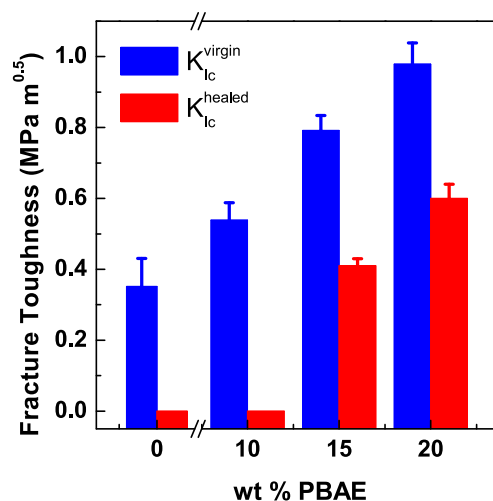

Fig. 6. Effect of increasing the wt % of PBAE on both virgin and healed fracture toughness for type I reference specimens. At low wt % PBAE, minimal toughening occurs and no healing was observed after injection of 5 μl of EPA and 2 d of heal time. With 20 wt % PBAE, the highest increase in virgin fracture toughness was observed and also the highest average healed fracture toughness.

Type I reference tests were conducted first to determine which loading of thermoplastic exhibited the maximum healing potential. Results are summarized in Fig. 6 and Table 2. In each reference test, 5 μl of EPA was manually injected into the fracture plane and the specimen was allowed to heal 2 d. During the allotted time, solvent locally dissolved the thermoplastic and redistributed it in the crack plane. Specimens with 20 wt % PBAE exhibited the greatest increase in fracture toughness as well as highest healing performance. Similar trends were observed for 15 wt % PBAE. No healing was observed for 10 wt % PBAE and the control case (0 wt % PBAE, control I). We suspect that 10 wt % PBAE was insufficient to produce a continuous healed film. For the control case, solvent was unable to heal the crack since the epoxy was fully cured.

3.4.2. Effect of microcapsules − autonomous healing

Microcapsules (5 wt %) were added to select specimens with 20 wt % PBAE to achieve an autonomous healing response. A summary of healing results compared to both type I and type II reference samples is presented in Fig. 7. The presence of microcapsules increased the virgin fracture toughness (Fig. 7a) of self-healing samples (26% compared to reference samples). Control III samples also exhibited toughening due to the addition of microcapsules, but no healing was observed without PBAE (Table 2).

As seen in Fig. 5, recovery of fracture toughness was dependent on healing time (Fig. 7b). Healing performance gradually increased to an average of 57% recovery after 6 days of healing time for self-healing specimens. A representative SEM image of a self-healing fracture surface after 6 days is shown in Fig. 8. False color (purple) was added to the healed film to show the redistribution of PBAE that occurred during the healing process and the tearing of the thermoplastic phase during the subsequent fracture.

The healing performance was compared to the response of type I reference tests, representative of the maximum healing potential for this system. The peak loads during the healed tests for both type I reference specimens and self-healing specimens were similar (i.e. capsule loading provided sufficient solvent to match the reference case), but the higher virgin fracture toughness of the microcapsule-filled self-healing specimens led to a lower overall healing efficiency. The capsule loading (5 wt %) was relatively low compared to prior work [20,21], but specimens prepared with 10 wt % capsules and did not exhibit an improvement in healing performance. For neat thermoplastic-toughened epoxy matrix (no microcapsules), the healing efficiency reached an average of 72%. In contrast to type I reference samples, control I specimens with no PBAE showed no
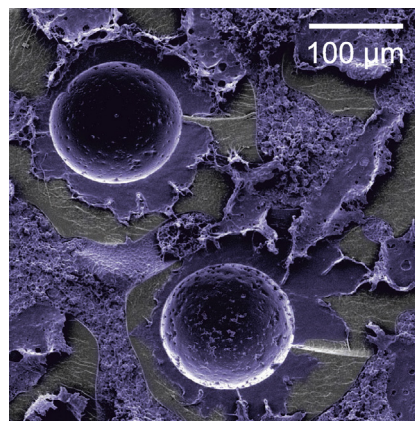

Fig. 8. Colorized SEM image (purple = PBAE healed film) of capsule filled fracture plane after both the virgin and healed test have been completed (6 day heal time). Tearing of the thermoplastic phase (purpled) is evident following the healed fracture event. (For interpretation of the references to color in this figure legend, the reader is referred to the web version of this article.)

recovery after 48 h at 30 °C, indicating that both PBAE and EPA are required for healing to occur.

The solvent-based healing system developed in the present work was compared with prior studies, in which heat was applied to achieve healing. A set of samples was exposed to both 130 °C for 1 h (in reference to prior work by Hayes et al. [11]) or 180 °C for 1 h (type II reference specimens). We observed no healing for samples exposed to 130 °C. We hypothesize that high healing efficiencies are only attainable if the material is heated near its glass transition temperature. Indeed, type II reference samples heated to 180 °C for 1 h achieved 67% recovery of fracture toughness. Control II samples (no PBAE, no capsules) showed zero recovery after the same healing cycle of 180 °C for 1 h.

3.4.3. Long term stability of healing performance

Self-healing samples were prepared and aged for up to 30 days at room temperature to evaluate the stability of the healing performance and microcapsules. In contrast to prior work by Caruso et al. [20], which relied on latent functionality of the matrix material, healing performance and fracture toughness remained stable after 30 days (Fig. 9). The lack of dependence on reactivity of encapsulated components makes this system an ideal candidate for long term aging studies.
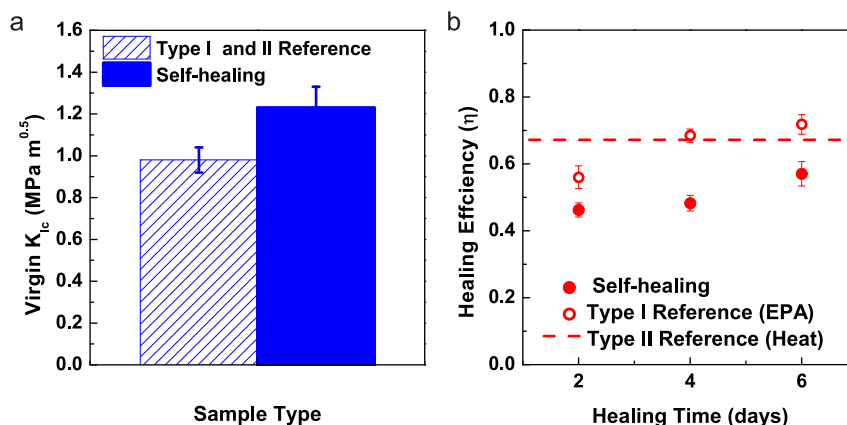

Fig. 7. Summary of healing performance for all sample types. (a) Virgin fracture toughness of self-healing specimens compared to reference samples. (b) Healing performance for all sample types. Self-healing specimens showed an increase in healing efficiency (up to 57%) with healing time, but at a slightly lower magnitude than reference tests (due largely to the increase in virgin fracture toughness for self-healing specimens). Type I and II references show similar behavior with healing efficiencies ca. 70%.
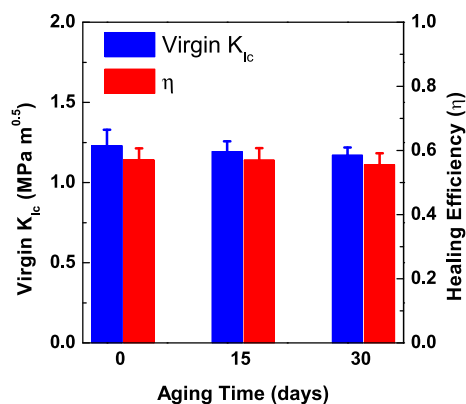
Fig. 9. Effect of aging time on healing performance for self-healing samples with 20 wt % PBAE. Healing efficiency and fracture toughness remained constant after aging at room temperature for 30 days.

4. Conclusions

A thermoplastic (PBAE)/solvent (EPA) healing chemistry was developed to overcome limitations of previous self-healing systems related to thermal stability during high performance epoxy cure cycles ($T_g > 150$ °C) and gradual loss of functionality of reactive encapsulates. The effect of the PBAE on epoxy mechanical properties and fracture toughness was investigated and used to select the optimum healing system. Microcapsules containing the solvent EPA were coated with a thin layer of poly(dopamine) and showed negligible loss of core content after 3 h at 180 °C. Reference tests, in which the solvent was manually injected into the fracture plane of a 20 wt % PBAE/epoxy, yielded an average healing efficiency of 72%. Fully autonomous healing tests, in which the solvent was delivered via rupture of embedded microcapsules yielded an average healing efficiency of 57%. This slight reduction in healing efficiency was due to an increase in virgin fracture toughness by the addition of 5 wt% microcapsules. Healed load—displacement response was similar for reference samples and self-healing samples, which indicated that similar healed films were developed in both cases. Samples showed no change in healing performance after aging at room temperature for up to 30 days.

References

[1] B. Blaiszik, S. Kramer, S. Olugebefola, J. Moore, N. Sottos, S. White, Self-healing polymers and composites, Annu. Rev. Mater. Res. 40 (2010) 179—211.
[2] H. Jin, C.L. Mangun, A.S. Griffin, J.S. Moore, N.R. Sottos, S.R. White, Thermally stable autonomic healing in epoxy using a dual-microcapsule system, Adv. Mater. 26 (2013) 1—6.
[3] C. Mangun, A. Mader, N. Sottos, S. White, Self-healing of a high temperature cured epoxy using poly(dimethyl siloxane) chemistry, Polymer 51 (2010) 4063—4068.
[4] H. Jin, C.L. Mangun, D.S. Stradley, J.S. Moore, N.R. Sottos, S.R. White, Self-healing thermoset using encapsulated epoxy-amine healing chemistry, Polymer 53 (2012) 581—587.
[5] H. Zhang, J. Yang, Development of self-healing polymers via amine-epoxy chemistry: I. Properties of healing agent carriers and the modelling of a two-part self-healing system, Smart Mater. Struct. 23 (2014a) 065003.
[6] H. Zhang, J. Yang, Development of self-healing polymers via amine-epoxy chemistry: II. Systematic evaluation of self-healing performance, Smart Mater. Struct. 23 (2014b) 065004.
[7] Y.C. Yuan, X.J. Ye, M.Z. Rong, M.Q. Zhang, G.C. Yang, J.Q. Zhao, Self-healing epoxy composite with heat-resistant healant, ACS Appl. Mater. Interf. 3 (2011) 4487—4495.
[8] R.A. Pearson, Toughening epoxies using rigid thermoplastic particles, in: C.K. Riew, A.J. Kinloch (Eds.), Toughened Plast, vol. 233, American Chemical Society, Washington, DC, 1993, pp. 405—425.
[9] J.H. Hodgkin, G.P. Simon, R.J. Varley, Thermoplastic toughening of epoxy resins: a critical review, Polym. Adv. Technol. 9 (1998) 3—10.
[10] R.J. Varley, D.A. Craze, A.P. Mouritz, C.H. Wang, Thermoplastic healing in epoxy networks: exploring performance and mechanism of alternative healing agents, Macromol. Mater. Eng. 298 (2013) 1232—1242.
[11] S. Hayes, F. Jones, K. Marshiya, W. Zhang, A self-healing thermosetting composite material, Compos. Part A 38 (2007) 1116—1120.
[12] X. Luo, R. Ou, D.E. Eberly, A. Singhal, W. Viratyaporn, P.T. Mather, A thermoplastic/thermoset blend exhibiting thermal mending and reversible adhesion, ACS Appl. Mater. Interf. 1 (2009) 612—620.
[13] K. Pingkarawat, C. Wang, R. Varley, A. Mouritz, Self-healing of delamination cracks in mendable epoxy matrix laminates using poly[ethylene-co-(methacrylic acid)] thermoplastic, Compos. Part A 43 (2012) 1301—1307.
[14] M.M. Caruso, B.J. Blaiszik, H. Jin, S.R. Schelkopf, D.S. Stradley, N.R. Sottos, S.R. White, J.S. Moore, Robust, double-walled microcapsules for self-healing polymeric materials, ACS Appl. Mater. Interf. 2 (2010) 1195—1199.
[15] S. Kang, S.R. White, N.R. Sottos, Core-shell polymeric microcapsules with superior thermal and solvent stability, ACS Appl. Mater. Interf. 7 (2015) 10952—10956.
[16] J.D. Rule, N.R. Sottos, S.R. White, Effect of microcapsule size on the performance of self-healing polymers, Polymer 48 (2007) 3520—3529.
[17] J. Hedrick, I. Yilgor, M. Jurek, J. Hedrick, G. Wilkes, J. McGrath, Chemical modification of matrix resin networks with engineering thermoplastics: 1. Synthesis, morphology, physical behaviour and toughening mechanisms of poly(arylene ether sulphone) modified epoxy networks, Polymer 32 (1991) 2020—2032.
[18] D. Hourston, J. Lane, The toughening of epoxy resins with thermoplastics: 1. Trifunctional epoxy resin-polyetherimide blends, Polymer 33 (1992) 1379—1383.
[19] J.L. Moll, H. Jin, C.L. Mangun, S.R. White, N.R. Sottos, Self-sealing of mechanical damage in a fully cured structural composite, Compos. Sci. Technol. 79 (2013) 15—20.
[20] M.M. Caruso, B.J. Blaiszik, S.R. White, N.R. Sottos, J.S. Moore, Full recovery of fracture toughness using a nontoxic solvent-based self-healing system, Adv. Funct. Mater 18 (2008) 1898—1904.
[21] S. Neuser, V. Michaud, S. White, Improving solvent-based self-healing materials through shape memory alloys, Polymer 53 (2012) 370—378.